Proceedings World Geothermal Congress 2020+1
Reykjavik, Iceland, April - October 2021

Numerical study of CO_2 based Enhanced Geothermal System at Chumathang Field, Ladakh, India

Sri Kalyan Tangirala[1], Mrityunjay Singh[2]

[1] Indian Institute of Technology (Indian School of Mines) Dhanbad, India; [2] Indian Institute of Technology Madras, India

E-mail address: [1] tangiralask@gmail.com; [2] 56mems@gmail.com

Keywords: Chumathang geothermal field, Enhanced Geothermal System, CO_2, Discrete fracture network

ABSTRACT

India has a vast amount of geothermal resources spread across its landmass. The high enthalpy resources are located close to the plate boundary of the Indian and Eurasian plates. Two of the most promising geothermal regions of India are the Puga and Chumathang geothermal fields. They lie on either side of the Indus Tsangpo suture zone, with the Chumathang field on its north and at an elevation of 3950 m from the mean sea level. Chumathang field has a geothermal gradient of around 80 °C/km. The Himalayan granites have high concentrations of U, Th, and K in addition to being on the plate boundary, which explains the high geothermal gradient in that region. Mahe fault lies close to the Chumathang field and helps in the percolation of fluids in and out of the field and also supplies a high heat flow rate. We numerically modeled a hot dry rock reservoir at a 2 km depth and away from the hydrothermally altered zone of the Chumathang field. Supercritical CO_2 was used as the heat transferring fluid due to its low reactivity and low viscosity. A connected discrete fracture network using LaGriT as the meshing software and PFLOTRAN as the heat and mass transport solver was used to study heat transport by injecting cold liquid CO_2 and producing hot supercritical CO_2 and water for estimating the energy extraction potential.

1. INTRODUCTION

Enormous amount of heat is being radiated from the inner parts of the Earth towards the surface and out into the atmosphere. However, geothermal energy is not as popular as solar or wind. Geothermal energy is one of the cleanest forms of energy out there. It emits very less amount of CO_2 in its entire lifecycle, that too only where there is geochemical activity in the hydrothermally altered areas or magma associated regions. On the other hand, solar photovoltaic cells emit a lot of CO_2 in their lifecycle (Chandrasekharam and Pathegama, 2020). In the present study, we are using CO_2 as the heat exchanging fluid by injecting it into the reservoir, so that our system can be considered as a carbon negative system as there is a high chance that some of it gets sequestered. Brown (2000) first suggested the idea of using supercritical CO_2 in place of water to extract geothermal energy from Hot Dry Rocks (HDR). The advantages and drawbacks of using supercritical CO_2 in place of water to extract heat from hot sedimentary and dry rock reservoirs has been reviewed in detail by Singh et al. (2020b). Considering the advantages of CO_2 like low reactivity and high mobility, in addition to part of it getting sequestered beneath the surface being environmentally friendly, we used CO_2 as the heat transmission fluid for our model.

India is rich in geothermal resources consisting of both hydrothermal and hot dry rocks (Granites). Extensive geothermal exploration in India has been done before the year 2000 where hydrothermally altered zones were identified and borehole studies were carried out in most of these zones. In mainland India, the most promising geothermal fields lie along the plate boundary of the Indian and Eurasian plates, mostly located in the Himalayan valleys at an elevation of around 4000 m above mean sea level. Puga and Chumathang fields (shown in Fig.1) are two of the most promising fields located in the Ladakh region at an altitude of 4400 m and 3950 m respectively. Chumathang geothermal system is also easier to access when compared to the Puga field. The entire region lies on the Ladakh batholith and a part of it is outcropped close to Chumathang. There is no existing literature demonstrating the geothermal heat extraction capacity of the Chumathang geothermal system from deeper hot dry rocks. These dry rocks may not comprise well connected fractures. Therefore, to extract energy from these rocks, hydraulic fracturing is necessary. In this work, we have numerically modeled the geothermal energy extraction from a network of fully connected fractured rock with rock properties based on the Chumathang field. We used CO_2 to transmit the heat through these fractures. We injected cold liquid CO_2 and produced hot supercritical CO_2. We also modeled the early drainage of water which was present in the fractures after hydraulic fracturing, using injected cold liquid CO_2.

A connected fracture network is the zone that allows to transfer heat from the hot dry rocks to the cold fluid. Kolditz (1995) numerically modeled the HDR system at Soultz, France for different cases and showed that when neighboring parallel arrays of fractures are connected with thermal interaction between them, the heat depletion in the reservoir quickens, but improves the longevity of the fracture network. Later, Chen and Jiang (2015) studied the effect of multiple wells in a homogeneously fractured hot dry rock reservoir where single values of permeability and porosity were used and water was injected as the heat exchanging fluid. They found a strong dependence of energy extracted with the layout of the wells and also mentioned that even for a heterogeneous reservoir, the well placement and longer fracture connectivity paths play a major role in increasing the amount of extractable energy. Makedonska et al. (2016) studied the effect of internal aperture variability in discrete fracture networks and concluded that it does not have a huge impact on fluid flow. Tang et al. (2020) modeled heat extraction using cold water and showed that if the fluid flows through a longer distance with low velocity and a small fracture width, high production temperatures can be achieved, whereas we can extract more geothermal energy with higher fluid velocities and larger fracture widths. Zeng et al. (2019) modelled a fractured heterogeneous Hot Dry Rock reservoir at Gonghe basin geothermal field by the Multiple Interacting Continua (MINC) method where the system had different permeabilities to calculate the amount of electricity generation. They used water as the heat exchanging fluid and showed that the reservoir heterogeneity has a considerable impact on the temperature distribution in the fracture families. The families with higher permeabilities would display a cold front which would disturb the even temperature flow. They also documented that the electricity generation capacity would reduce with increase in fracture spacing. Recently, Liu et al. (2020) modeled a discrete fracture network system where water was the heat exchanging fluid at Sanguliu granite in the Liaodong Peninsular region in Eastern China, where they showed that if the matrix had higher permeability and porosity, then the time taken for thermal breakthrough is increased. They also showed that fractures with large apertures are good conduits for fluids when compared to fractures with small apertures. Makedonska et al. (2020) modelled a discrete fracture network at the EGS Collab testbed at Sanford Underground Research Facility (SURF) and reported that the fluid prefers to travel through the hydraulically stimulated fractures from the injection to production well via the shortest distance, irrespective of the network fracture intensity.

Use of CO_2 for geothermal energy extraction has various benefits. Brown (2000) was the first to suggest that CO_2 could be used instead of water in geothermal systems. Pruess and Azaroual (2006) studied the feasibility of using $ScCO_2$ as the heat exchanging fluid through a horizontal fracture space in an engineered hot dry rock geothermal system and concluded that CO_2 is comparable with water and in some cases, even better than it. Due to its buoyancy, $ScCO_2$ reduces the power needed to maintain the circulation of fluids in the well. A study by Liu et al. (2017) investigated that a lower flow rate between the injection and production wells produces CO_2 of higher temperature when compared to a higher flow rate between the wells at the HDR geothermal field of Zhacanggou, China by modeling the system as a porous media with a permeability of 10^{-13} m^2 and a porosity of 0.2. Shi et al. (2018) used $ScCO_2$ for fracturing the domain, so the fractures are filled with the same fluid before injection. The reservoir they modeled contained random natural fractures and discrete fracture networks in connection to them, where flow started and ended at multilateral wells. They reported that the injection rate and production pressure showed a great impact on CO_2 - EGS performance. They concluded that multilateral wells showed better heat extraction when compared to regular doublet systems. Hyman et al. (2020) modeled the displacement of water by supercritical CO_2 in a 3-D discrete fracture network using dfnWorks for fracture generation and FEHM for fluid flow. They injected $ScCO_2$ from the bottom face of the considered domain. For the case with low fracture density, the $ScCO_2$ could not flow through the hanging fractures due to its buoyancy. However, when the fracture density was significantly increased, it was flowing through them due to increased connectivity. They concluded that the network properties like fracture density have a more significant effect on the flow of $ScCO_2$ than the permeability of the individual fractures in a less dense network.

2. GEOLOGY

Geographically, Chumathang is located in the Ladakh region of India. Puga and Chumathang lie on either sides of the Indus Tsangpo suture zone, with Chumathang to its north and Puga to its south. Chumathang is situated in the Himalayas which were formed as a result of collision of the Indian and Eurasian plates. The Ladakh granite, locally known as Chumathang granite (batholith) intrudes the sedimentary sequence and it is exposed around 3.6 km east of Chumathang along the east of the Indus river (St-Onge et al. 2010). The Indus suture zone actually represents the zone of collision of Indian and Eurasian plates.

Most of the literature refers to the hydrothermally altered zone of the Chumathang geothermal field. This region has 73 hot springs in an area of around 1 sq.km. The entire Chumathang region is covered with granites of high concentrations of U, Th and K. Pinet and Jaupart (1987) reported high concentration of U, Th and K in the Manaslu granites of Nepal. During the collision of Indian and Eurasian plates, a Transhimalayan calc-alkaline batholith of 2500 km in length was formed along the collision zone. That batholith majorly comprises biotite and hornblende bearing granodiorite, gabbro and evolved biotite granite (St-Onge et al. 2010). Since the granites at Manaslu, Ladakh, and most of them along the plate boundary were formed more or less around the same time and by the same mechanism, we assumed that there wouldn't be a drastic difference in U, Th and K concentration values between Manaslu and Chumathang.

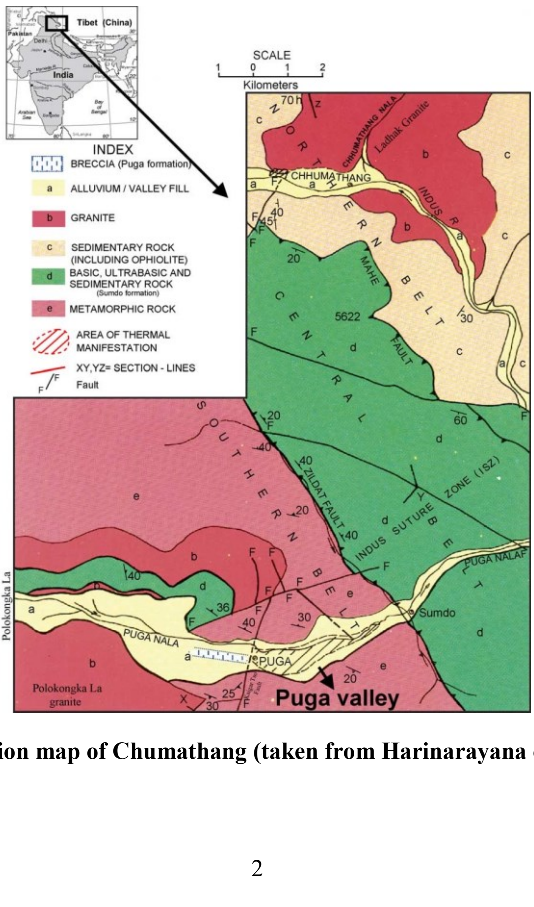

Fig. 1 Location map of Chumathang (taken from Harinarayana et al. 2004)

The shaded regions in Fig. 1 indicate the thermally manifested zones comprising many hot springs. The enhanced geothermal system we chose to model was selected in the Ladakh granite, shown in red in Fig.1. The geologic cross section of the Indus Tsangpo Suture Zone (ITSZ) is shown in Fig. 2. It shows the main thrusts on the Indian plate as well as the location of Puga and Chumathang fields.

Thussu and GSI (2002) reported that the thermally manifested zone of the Chumathang geothermal field has around 73 hot springs of temperatures varying between 30 °C to 87 °C. Borehole studies showed highly anomalous geothermal gradients like 0.7 °C/m - 2.5 °C/m within the depths of 20 m - 221 m. Thermal waters with a maximum of 109 °C were encountered by the boreholes.

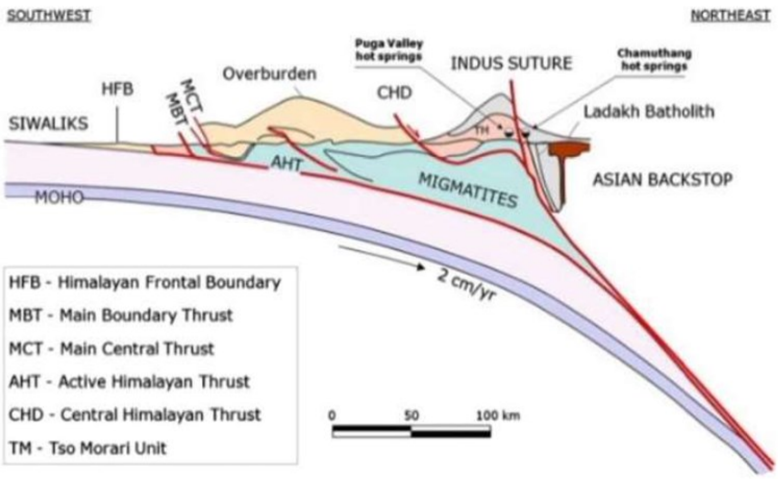

Fig. 2 Geologic cross section of the Indus Tsangpo Suture Zone(ITSZ) (taken from Rawat et al. (2020))

The anomalous gradients are due to the presence of different kinds of strata having different thermal conductivities and can't be applied in other regions where the rock type is different. Various chemical geothermometers suggested temperatures between 145 °C and 184 °C for the deep reservoir (Thussu and GSI, 2002). However, these borehole studies were not deep enough to investigate the deeper penetration into the granites. The granites present below these thermally altered zones may have much higher geothermal energy potential at deeper depths.

3. MATHEMATICAL AND NUMERICAL MODELING

The theoretical predictions for geothermal energy extraction from the hot dry rocks (HDR) at Chumathang geothermal field are modeled using a three-dimensional discrete fracture network modelling suite dfnWorks (Hyman et al. 2015). We stochastically generated a network of three dimensional fractures with the help of Feature Rejection Algorithm for Meshing (FRAM) (Hyman et al. 2014) and used LaGriT meshing toolbox (LaGriT 2013) for meshing the generated fractures. FRAM and LaGriT were integrated into dfnWorks along with PFLOTRAN (Lichtner et al. 2015), a parallel heat and mass transport solver, which was used to simulate the multiphase flow of water with liquid and $ScCO_2$.

We considered that the stochastically generated network of fractures in the HDR were filled with water (from hydraulic fracturing) and was displaced by cold liquid CO_2. The thermodynamic properties of CO_2 in comparison to water for a wide range of temperatures are shown in Fig. 4 of our previous work (Singh et al. 2020b). The mechanisms of injected CO_2 (cold liquid CO_2) in HDR are governed by coupled macroscopic mass balance equation, Darcy flow equation for both water and $ScCO_2$, and heat transport equation, which were taken from Singh et al. (2020a).

$$\frac{\partial}{\partial t}(\phi\sum_\alpha \rho_\alpha C_{\beta,\alpha} S_\alpha) + [\frac{\partial}{\partial x}(\sum_\alpha \rho_\alpha C_{\beta,\alpha}\boldsymbol{q}_\alpha) + \frac{\partial}{\partial z}(\sum_\alpha \rho_\alpha C_{\beta,\alpha}\boldsymbol{q}_\alpha)] - [\frac{\partial}{\partial x}(\phi\sum_\alpha \rho_\alpha S_\alpha D_{\beta,\alpha}\frac{\partial}{\partial x}C_{\beta,\alpha}) + \frac{\partial}{\partial z}(\phi\sum_\alpha \rho_\alpha S_\alpha D_{\beta,\alpha}\frac{\partial}{\partial z}C_{\beta,\alpha})] = 0 \quad (1)$$

$$\boldsymbol{q}_{x,\alpha} = -\frac{k k_{r,\alpha}}{\mu_\alpha}(\frac{\partial P_\alpha}{\partial x}) \quad (2)$$

$$\boldsymbol{q}_{z,\alpha} = -\frac{k k_{r,\alpha}}{\mu_\alpha}(\frac{\partial P_\alpha}{\partial z} - \rho_\alpha \boldsymbol{g}) \quad (3)$$

In the above equations α and β represent fluid phase and component respectively. Here $\alpha = w$ for wetting phase fluid i.e. water and $\alpha = nw$ for non-wetting phase fluid i.e. supercritical/liquid CO_2. The symbols ρ_α, S_α, $\boldsymbol{q}_\alpha$, p_α, μ_α, and $k_{r,\alpha}$ are used for density (kg/m^3), saturation, volumetric flux (m^3/(m^2 s)) (Darcy flux), pressure (Pa), viscosity (Pa.s) and relative permeability of fluid phase α, respectively. Reservoir permeability and Porosity are denoted by k and ϕ, respectively. The mass fraction of component β in fluid phase α is denoted as $C_{\alpha,\beta}$, and $D_{\alpha,\beta}$ is the corresponding diffusion coefficient. Here β can be CO_2 or W corresponding to CO_2 or water, respectively. The saturation and mass fractions satisfy the following conservation laws.

$$S_w + S_{nw} = 1, C_{CO_2,w} + C_{W,w} = 1 \; and \; C_{CO_2,nw} + C_{W,nw} = 1 \quad (4)$$

The energy balance equation for multiphase flow in porous medium is given as,

$$\frac{\partial}{\partial t}((1-\phi)\rho_s C_{ps}T + \sum_{\alpha}\phi(\rho_\alpha S_\alpha C_{p\alpha}T)) + [\frac{\partial}{\partial x}(\phi\sum_{\alpha}\rho_\alpha S_\alpha \boldsymbol{q}_\alpha H_\alpha) + \frac{\partial}{\partial z}(\phi\sum_{\alpha}\rho_\alpha S_\alpha \boldsymbol{q}_\alpha H_\alpha)] - [\frac{\partial}{\partial x}(\lambda_m \frac{\partial T}{\partial x}) + \frac{\partial}{\partial z}(\lambda_m \frac{\partial T}{\partial z})] = 0 \tag{5}$$

In the above equation T is temperature, C_{ps} and $C_{p\alpha}$ are the heat capacity of solid and fluid phase α. H_α is the enthalpy of fluid phase α, and λ_m is the effective thermal conductivity of the medium. Subscript s corresponds to solid phase.

For a two phase fluid system, relative permeability of a fluid phase in a saturated reservoir is the effective permeability of that phase at some saturation with respect to the absolute permeability at total saturation. We have used the van Genuchten function to model relative permeability (Genuchten 1980).

The van Genuchten saturation function based Burdine relative permeability function can be expressed as

$$k_{r,w} = \hat{S}^2\{1-[1-(\hat{S})^{n/(n-2)}]^{(1-2/n)}\} \tag{6}$$

The van Genuchten constitutive relations for capillary pressure and saturation is,

$$P_{nw} - P_w = p_{c_0}[\hat{S}^{-1/n} - 1]^{1-n} \tag{7}$$

In the above equations (Eq. 6 and Eq. 7), S is the effective water saturation and it is defined as $S = (S_w - S_{rw})/(1-S_{rw})$. S_{rw} is residual water saturation. Here n is the van Genuchten exponent value and $\boldsymbol{g}$ is the gravitational acceleration vector ($-9.81k$ m/s^2). We have ignored the effect of $\boldsymbol{g}$ in the present study and will consider it in our future work. Here, p_{c0} is the capillary entry pressure.

The axial origin of our hot dry rock model considered is 2 km below the earth's surface, and since the permeability and porosity of granite is very low, it acts as both bedrock and caprock. We considered a domain of volume 50 m x 50 m x 50 m with a depth of 1975 m at the top and 2025 m at the bottom. The properties of the hot dry rock system are listed in Table 1. A periodic boundary condition was applied to the sides of the domain. The injection and production wells are penetrating throughout the entire depth of our domain and are located diagonally opposite to each other at a distance of 56.56 m. The CO_2 injection mass flow rate of 1.6 kg/s and production pressure was maintained at 1 MPa below the pore pressure. The CO_2 was injected into the reservoir in liquid phase and at 25 ^{O}C. The initial local temperature in the vicinity of the injection well was 156 ^{O}C. The run time of the simulation was 5 years.

Table 1: Domain properties used for simulation

Domain properties	Values
Region	50 m x 50 m x 50m
Geothermal gradient	78 ^{O}C/km (Thussu and GSI, 2002)
Thermal conductivity	2.3 W/mK (Pinet and Jaupart, 1987)
Porosity	0.001
Rock density	2690 kg/m^3
Specific heat capacity	900 J/kgK (Hartlieb et al. 2016)

Fig. 3 shows the three dimensional meshed discrete fracture network we used for our simulations. A total of 99 elliptical fractures (in two families) were generated stochastically by the truncated power law. The fracture intensity was assigned to be p32 = 0.5 for both the families. The fractures were generated such that all the faces of the cubic domain were individually intersected by at least some fractures. Both the families are assigned a fracture intensity of 0.5 each. The permeability and aperture of all fractures are assigned to be constant and the values are 1x10^{-12} m^2 and 1x10^{-5} m respectively. We assumed that there would be no triple intersecting fractures in the domain.

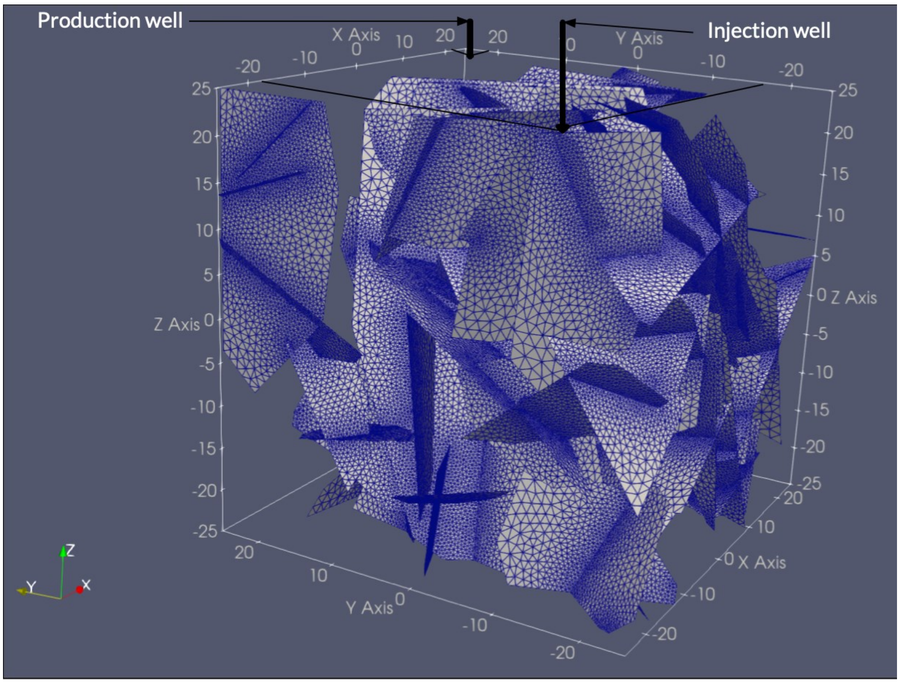

Fig. 3 A Discrete Fracture Network consisting of 99 fractures in a 50 meter cube domain, where the positions of the injection and production wells are also labelled.

4. RESULTS

In this work, we studied CO_2 driven water drainage from a discrete fracture network in a hot dry rock. The mechanism of drainage and the effect of multiphase fluid and heat transport in the fracture networks are the main features of this study. The system we considered had very less matrix porosity and permeability, so we ignored the flow through the matrix. Here, the fluid flow occurs through the connected fractures only. Non-connected fractures are not present in the domain. The fractures in the hot dry rock are initially filled with water left from the hydraulic fracturing. Figure 4 shows the CO_2 saturation in water, HDR temperature (in °C) and liquid energy (in MJ/kmol) remaining in the HDR system. The saturation near the injection well is 0.9 in some regions immediately next to the injection well, close to 0.8 in parts little away from the injection well, and less than 0.01 near the production well (see Fig. 4(A, D, G & J)). As soon as we inject high density liquid CO_2, its temperature increases, phase transition occurs and liquid CO_2 becomes supercritical CO_2. As the CO_2 injection begins, the saturation of supercritical CO_2 in water increases much faster than the drop in the HDR temperature as shown in Fig. 4A and 4B. In this model, we injected approximately 0.25 million tonnes of liquid CO_2 and produced approximately 1.6 thousand tonnes of supercritical CO_2 in a duration of five years. The production temperature was maintained at 156 °C and the production well was maintained at 1 MPa below the pore pressure, i.e. at 18.75 MPa. Due to the predefined pressure boundary condition, we were able to produce 3.42 million tonnes of water from the fracture network. This very high production mass can be attributed to the open boundaries from all the sides. Cumulatively, we estimated that from the present HDR system, we can generate 2.29 PJ of energy within five years of the commencement of the injection only from water, and 0.87 TJ can be produced through injected CO_2. This translates to 14.5 MW of power for five years. However, the proportion of heat extraction through CO_2 increases with time as more fractures get completely saturated with the CO_2.

Comparing Fig. 4 (D, G, & J) and Fig. 4 (E,H & K), it is clearly evident that after the initial faster saturation spread in the fracture network, the temperature drop in the fracture network follows the free phase CO_2 propagation. The liquid energy represents the energy available with the water present in the fractures as shown in Fig. 4 (C, F, I & L). The thermal depletion of the rock is due to the cold injection of CO_2 and after five years, only a small fraction of the whole rock system's temperature has dropped up to the cold CO_2 injection temperature. Also, from the liquid energy distributions, we can easily interpret that there is enough energy remaining in the hot dry rock even after five years of energy extraction. More longer and complex simulations would be published in our future work. The fracture temperature in the vicinity of the production well has not dropped below the initial HDR temperature even after 5 years of fluid transmission showing a very slow cold thermal front propagation in the fracture network. Therefore, such fracture networks may support longer geothermal heat extraction projects.

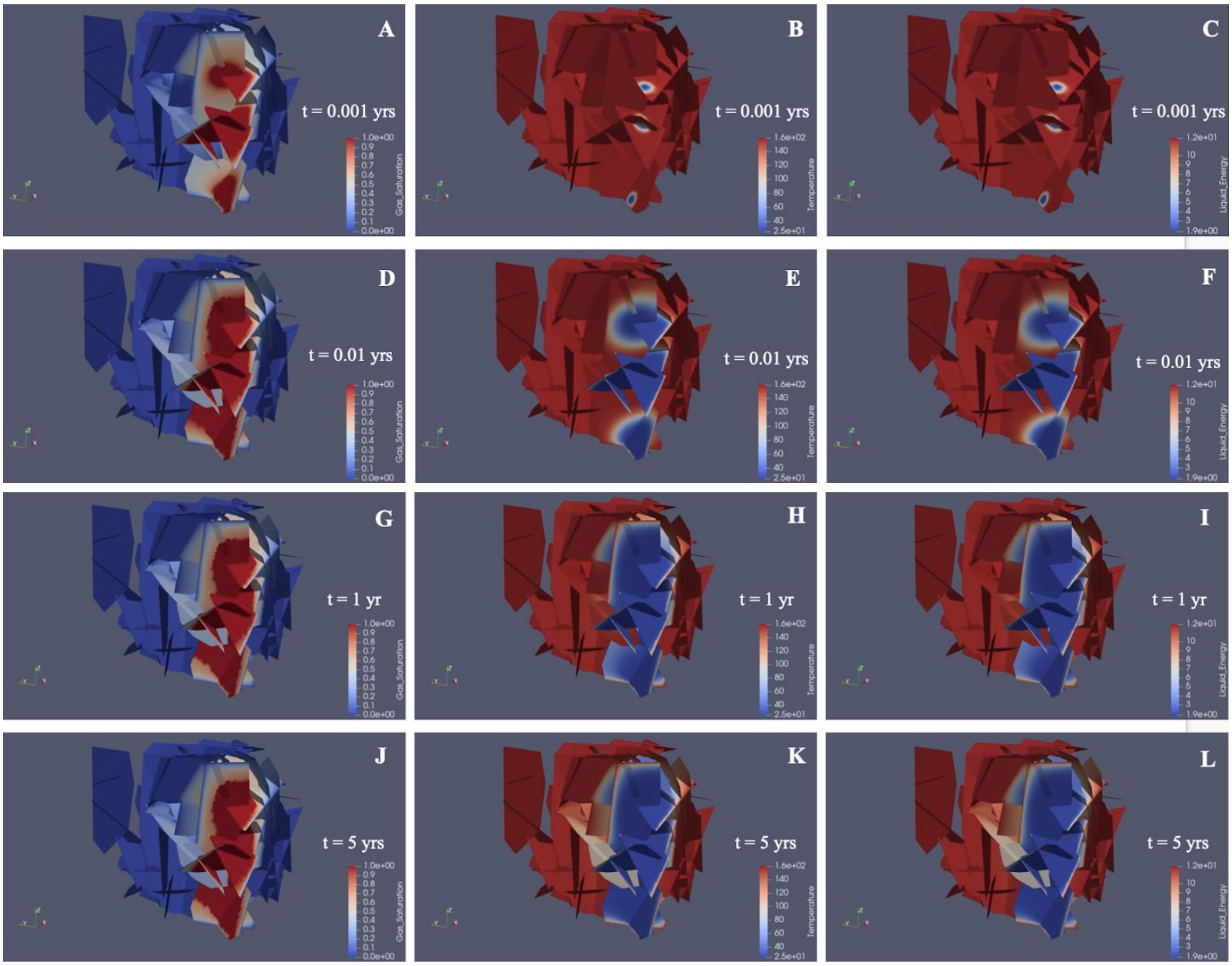

Fig. 4 (A, D, G and J) Saturation of liquid and ScCO$_2$, (B, E, H and K) temperature (in °C) of the HDR system, and (C, F, I and L) the remaining liquid energy (in MJ/kmol) in the fracture network.

5. CONCLUSIONS

A three dimensional fully connected discrete fracture network in a hot dry rock system was modeled in this study to estimate the geothermal energy extraction potential at the Chumathang field, Ladakh, India. We created a system of fully connected elliptical fractures in this model. The thermal drawdown and multiphase fluid dynamics were investigated in this study. The major outcome of this study is to model complex two phase fluid dynamics in a fracture network and heat transmission through the two-fluid system. We also estimated the minimum energy production in a span of five years from a small domain in hot dry rocks of the Chumathang field to be 2.29 PJ. This means that we can generate 14.5 MW of power for 5 years. We found that the free phase CO_2 spread is much faster than the thermal depletion in a fracture network and five years is not sufficient to completely drain water from a network of fractures present between two wells placed 56.56 m apart. Since our model was just a small volume of 50 meter cube, the amount of energy that is stored in that region is enormous and we need longer duration simulations in a larger domain to predict the maximum possible fluid drainage time and true potential of the hot dry rocks in the entire region.

6. ACKNOWLEDGEMENTS

The authors gratefully acknowledge Dr. Abhijit Chaudhuri for providing the computational facility of his lab at Indian Institute of Technology Madras, India. We would also like to thank Prof. Dornadula Chandrasekharam from Indian Institute of Technology Hyderabad, India for his invaluable inputs about the Chumathang geothermal field. We also thank Dr. Jeffrey Hyman of Los Alamos National Laboratory for his assistance with dfnWorks packages.

REFERENCES

Brown D. A hot dry rock geothermal energy concept utilizing supercritical CO_2 instead of water. In 25th workshop on geothermal reservoir engineering. Stanford University, (2000), Stanford. SGP-TR-165.

Chandrasekharam, D., Ranjith Pathegama, G., CO_2 emissions from renewables: solar pv, hydrothermal and EGS sources. *Geomech. Geophys. Geo-energ. Geo-resour.* 6**,** 13 (2020). https://doi.org/10.1007/s40948-019-00135-y

Chen, J., Jiang, F., Designing multi-well layout for enhanced geothermal system to better exploit hot dry rock geothermal energy, Renewable Energy, 74, 37-48, (2015), https://doi.org/10.1016/j.renene.2014.07.056.

Christophe Pinet, Claude Jaupart, A thermal model for the distribution in space and time of the Himalayan granites. Earth and Planetary Science Letters, 84 (1), 87-99, (1987), https://doi.org/10.1016/0012-821X(87)90179-8.

Harinarayana, T., Azeez, Abdul, Naganjaneyulu, K.K., Manoj, K., Veeraswamy, C., Murthy, K., Prabhakar Eknath, D.N., Rao, S. Magnetotelluric studies in Puga valley geothermal field, NW, Himalaya, Jammu and Kashmir, India. J. Volcanol. Geotherm. Res. 138, 405–424, (2004), http://dx.doi.org/10.1016/j.jvolgeores.2004.07.011.

Hartlieb, P., Toifl, M., Kuchar, F., Meisels, R., Antretter, T., "Thermo-physical properties of selected hard rocks and their relation to microwave-assisted comminution." Minerals Engineering, 91, 34-41, (2016), https://doi.org/10.1016/j.mineng.2015.11.008.

Hyman, J.D., Gable, C.W., Painter, S.L., Makedonska, N.: Conforming Delaunay triangulation of stochastically generated three dimensional discrete fracture networks: a feature rejection algorithm for meshing strategy. SIAM J. Sci. Comput. 36(4), A1871–A1894, (2014).

Hyman, J. D., Karra, S., Makedonska, N., Gable, C. W., Painter, S. L., & Viswanathan, H. S. dfnWorks: A discrete fracture network framework for modeling subsurface flow and transport. Computers & Geosciences, 84, 10-19, (2015).

Hyman, J.D., Jiménez-Martínez, J., Gable, C.W. *et al.* Characterizing the Impact of Fractured Caprock Heterogeneity on Supercritical CO_2 Injection. *Transp Porous Med* 131**,** 935–955, (2020). https://doi.org/10.1007/s11242-019-01372-1

Kolditz, O., Modelling flow and heat transfer in fractured rocks: Conceptual model of a 3-D deterministic fracture network, Geothermics, 24, 3, 451-470, (1995), https://doi.org/10.1016/0375-6505(95)00020-Q.

LaGriT: Los Alamos Grid Toolbox. (LaGriT) Los Alamos National Laboratory, Los Alamos (2013)

Lichtner, P. C., Hammond, G., Lu, C., Karra, S., Bisht, G., Andre, B., Mills, R. T., Kumar, J. "PFLOTRAN User Manual: A Massively Parallel Reactive Flow and Transport Model for Describing Surface and Subsurface Processes." *Technical Report No. LA-UR-15-20403, Los Alamos National Laboratory, Los Alamos, NM, USA*. (2015).

Liu, Y., Wang, G., Yue, G., Lu, C., Zhu, X. Impact of CO_2 injection rate on heat extraction at the HDR geothermal field of Zhacanggou, China. Environ Earth Sci 76 (6):1–11, (2017).

Liu, H., Wang, H., Lei, H., Zhang, L., Bai, M., Zhou, L,. "Numerical modeling of thermal breakthrough induced by geothermal production in fractured granite." Journal of Rock Mechanics and Geotechnical Engineering, 12, 4, 900-916, (2020), https://doi.org/10.1016/j.jrmge.2020.01.002.

Makedonska, N., Hyman, J.D., Karra, S., Painter, S.L., Gable, C.W., Viswanathan, H.S., "Evaluating the effect of internal aperture variability on transport in kilometer scale discrete fracture networks," Advances in Water Resources, 94, 486-497, (2016), https://doi.org/10.1016/j.advwatres.2016.06.010.

Makedonska, N., Jafarov, E., Doe, T., Schwering, P.C., Neupane, G., and EGS Collab Team: Simulation of injected flow pathways in geothermal fractured reservoir using discrete fracture network model, In 45th Workshop on Geothermal Reservoir Engineering, Stanford, CA, (2020).

Pruess, K., Azaroual**,** M., On the feasibility of using supercritical CO_2 as heat transmission fluid in an engineered hot dry rock geothermal system, Proceedings of the Thirty-First Workshop on Geothermal Reservoir Engineering at Stanford University, pp. 386-393, (2006).

Rawat G., Bartarya S.K., Singh B., Bhasin R.K. Geophysical Characterization of Chumathang (Ladakh) Hot Spring. In: Biswas A., Sharma S. (eds) Advances in Modeling and Interpretation in Near Surface Geophysics. Springer Geophysics. Springer, Cham. (2020), https://doi.org/10.1007/978-3-030-28909-6_13

Shi, Y., Song, X., Shen, Z., Wang, G., Li, X., Zheng, R., Geng, L., Li, J., Zhang, S. Numerical investigation on heat extraction performance of a CO2 enhanced geothermal system with multilateral wells, Energy, 163, 38-51, (2018), https://doi.org/10.1016/j.energy.2018.08.060.

Singh, M., Chaudhuri, A., Stauffer, P. H., & Pawar, R. Simulation of gravitational instability and thermo-solutal convection during the dissolution of CO_2 in deep storage reservoirs. *Water Resources Research*, *56*, e2019WR026126. (2020a). https://doi.org/10.1029/2019WR026126

Singh, M., Tangirala, S.K. & Chaudhuri, A. Potential of CO_2 based geothermal energy extraction from hot sedimentary and dry rock reservoirs, and enabling carbon geo-sequestration. Geomech. Geophys. Geo-energ. Geo-resour. 6, 16, (2020b). https://doi.org/10.1007/s40948-019-00139-8

St-Onge, M.R., Rayner, N., Searle, M. "Zircon age determination for the Ladakh batholiths at Chumathang (North-West India): Implications for the age of the India-Asia Collision in the Ladakh Himalaya". Tectonophysics, 495, 171- 183. (2010).

Tang, Y., Ma, T., Chen, P. *et al.* An analytical model for heat extraction through multi-link fractures of the enhanced geothermal system. *Geomech. Geophys. Geo-energ. Geo-resour.* 6**,** 1 (2020), https://doi.org/10.1007/s40948-019-00123-2.

Thussu. J.L. and Geological Survey of India, Geothermal Energy Resources of India. ISSN- 0254-0436, (2002).

van Genuchten, M.T. A Closed-form equation for predicting the hydraulic conductivity of unsaturated soils. Soil Sci. Soc. Am. J. 44:892–898, (1980), https://doi:10.2136/sssaj1980.03615995004400050002x

Zeng, Y.; Tang, L.; Wu, N.; Song, J.; Zhao, Z. Numerical Investigation of Influence of Reservoir Heterogeneity on Electricity Generation Performance of Enhanced Geothermal System. *Processes*, *7*, 202, (2019).